Denis Sacha

Microstructural Tests and Hardness Tests of Surface Layers of Nodular Cast Iron GJS-350 Made Using the Laser Surface Alloying Process

Abstract: The article presents test results concerning the microstructure and the hardness of a composite layer made on a substrate of nodular cast iron GJS-350 using the laser surface alloying method. The alloying agent used in the test was powdered titanium. The study consists of an overview of reference publications aimed to introduce the most important aspects concerning the issue subjected to analysis. The research part presents the methodology of tests as well as their results and analysis. Microscopic analysis revealed that the layer structure was fine-grained and highly homogenous, whereas hardness measurements revealed that the titanium-enriched layer was characterised by significantly higher micro-hardness than that of the base material.

Keywords: laser surface alloying, ductile cast iron, nodular cast iron, titanium carbide, in-situ composite

DOI: *10.17729/ebis.2021.6/4*

Introduction

Recent years have seen a true renaissance of nodular cast iron. The material is enjoying increasing popularity, particularly in the machine-building industry [1–3]. Nodular cast iron is characterised by favourable technological (castability and machinability) as well as mechanical properties, sometimes equalling those of carbon steels and cast steels [2–4]. In addition, in comparison with steels and cast steels, nodular cast iron is characterised by more favourable vibration damping ability, thermal conductivity and lower density [3]. However, in spite of the above-presented unquestionable advantages, the abrasive wear resistance of nodular cast iron proves overly low for the material to be used, e.g. in sleeves, valves etc. [2, 4]. The aforesaid problem can be addressed using increasingly common laser surface processing methods such as laser remelting or laser alloying [1–5]. Because of its effectiveness, a particularly promising method is the laser alloying of surface layers, enabling the obtainment of original structures using small amounts of alloying agents. An undeniable advantage of the method is the possibility to use a wide range of alloying agents, which translates into many various surface layer modifications [1–3]. Titanium additions are particularly useful in cases of elements which should be characterised by high abrasive wear resistance [1, 2]. The high content of carbon (in nodular cast irons)

inż. Denis Sacha, trainee at Łukasiewicz Research Network – Instytut Spawalnictwa, Department for Non-Destructive Tests

and its affinity for titanium enable the obtainment of composite-reinforced abrasive wear resistance layers, where the reinforcing phase is titanium carbide (formed as a result of the alloying process) [1].

Laser alloying of nodular cast iron with titanium

The alloying of surface layers of cast irons aims to improve their corrosion resistance and tribological properties [1–5]. The alloying process usually involves grey cast irons and high-strength cast irons and their enrichment with such powders as Fe-Si, B, Si, Cr, Ni (and its alloys) and C [6]. Another popular agent (recently) is titanium as it enables the making of very hard and abrasion resistant composite-reinforced surface layers [1, 2].

Laser surface alloying

The laser alloying (enrichment) of surfaces is a relatively new thermoplastic processing method involving the enrichment of surface layers with alloying agents. The method makes it possible to provide both small and large areas with w wide range of alloying agents. The enrichment of surface layers may involve the injection ("blowing") of powder, chemically active gases or the melting of the substrate, onto which an alloying agent (in the form of metal strips or electrolytic coatings) has been (previously) deposited. During the process, the base material and the alloying agent are simultaneously melted and mixed (as a result of convective movements and shielding gas pressure). Afterwards, mixed materials crystallise intensely and are cooled to ambient temperature [6]. The schematic diagram of the laser alloying process is presented in Figure 1.

As can be seen in Figure 1, there are two types of laser alloying, i.e. fusion and melting. The fusion process consists in the deposition of an alloying agent in a compact form (e.g. foil, galvanic coating, plates, strips etc.) or in the form of a porous layer (in the solid state, e.g. powder paste) on the base material and their simultaneous melting. In turn, the process of melting consists in providing the liquid metal pool with an alloying agent in the form of a wire, powder or gases [6].

The alloying process is applied to process metals and their alloys (primarily steels and grey cast irons), usually using single chemical elements. The process aims to improve specific properties of surface layers (e.g. abrasive wear resistance, heat resistance, corrosion resistance etc.). Materials (additions) enriching surface layers include non-metals (B, Si, N, C),

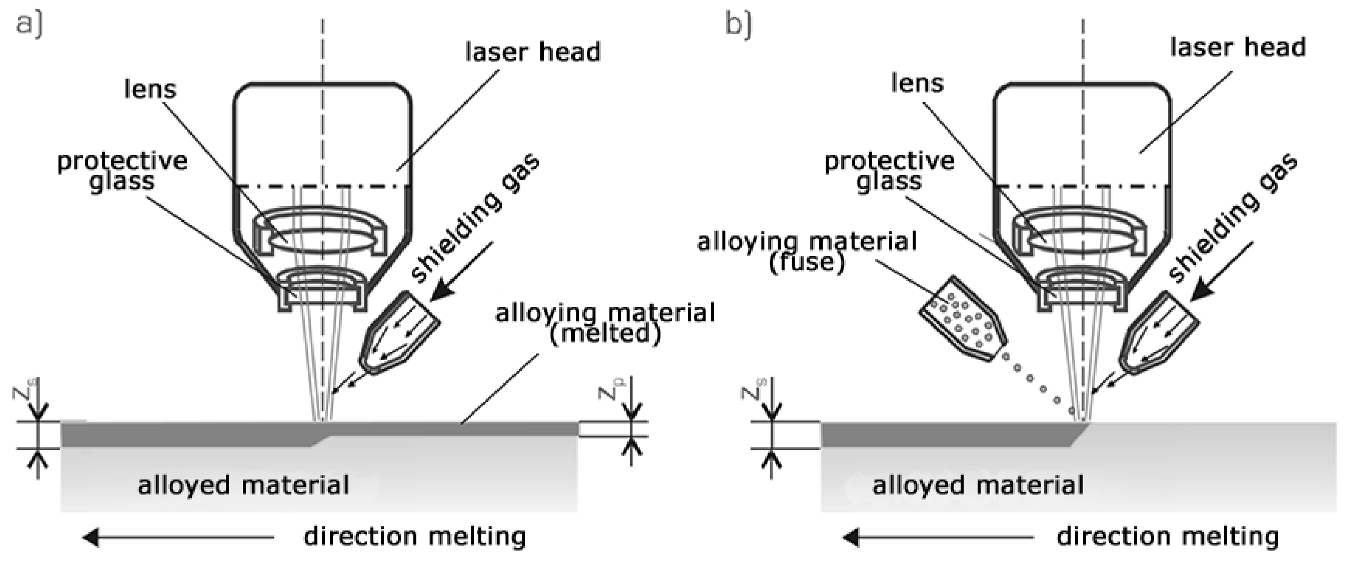

Fig. 1. Laser surface alloying: a) with an alloying addition previously deposited on the substrate (fusion) and b) with powder injected into the liquid metal pool (melting) [7]

metals or their alloys (np. Cr, Mn, Ti, Nb, V, Mo, etc.), gases (e.g. acetylene) and various compounds (primarily carbides e.g. TiC, Ni-Cr, WC, etc.) [6].

The laser alloying method is regarded as very effective and enables the obtainment of the following properties of surface layers [6]:
- high wear and erosion resistance,
- increased static and fatigue strength,
- high resistance to various types of corrosion, including high-temperature corrosion and corrosion in aggressive environments,
- specific physical properties of surfaces,
- decorative aspects.

The application of the laser beam distinguishes the laser alloying method from other thermoplastic treatment methods. The use of the laser leads to the obtainment of many favourable structural and practical results [6], i.e.:
- obtainment of alloyed layers of thicknesses restricted within the range of 0.3 mm to 3 mm,
- easy process automation,
- obtainment of the fine-crystalline structure,
- precise control of power density and its distribution,
- possibility of obtaining new materials containing metastable phases and supersaturated solid solutions.

Similar to laser surface hardening, laser alloying can be performed in one or several runs (in cases of larger areas) [6]. In the alloying process, the overlapping of neighbouring paths overlap has a favourable effect as it improves the homogenisation of the structure (more uniform distribution of products formed through the dilution of an alloying agent with the base material (e.g. carbides, nitrides etc.) [1].

In-situ composites

During the production of in situ method-based composites, the reinforcing phase is formed in the entire matrix as a result of an initiated and controlled chemical reaction [8, 9]. The reinforcement is obtained through nucleation and growth from the matrix, leading to the obtainment of various oxides, borides, carbides, nitrides, etc. [9].

The advantages of in-situ (as opposed to ex situ) composite materials are, primarily, the pure (non-oxidised) surface on the reinforcement-matrix boundary (providing stronger interphase bonds) and the high thermal stability of reinforcement particles formed in the matrix [1, 8]. The above-named advantages are responsible for favourable physicochemical properties of in situ composites such as high fatigue strength, thermal stability and abrasion resistance [1].

Titanium carbide

Titanium carbide (TiC) is an inorganic chemical compound characterised by a high melting point (approximately 3523 K), low density (approximately 4.9 g/cm^3), high hardness (approximately 3200 HV), high abrasion resistance and resistance to thermal shocks [10, 11]. Because of its favourable tribological properties, TiC is used as a component in tool ceramics, particularly in high-speed machining tools [10, 11]. In addition, titanium carbide is used in various protective coatings and as a reinforcing phase in composite materials and layers requiring high abrasion resistance, e.g. layers of grey and nodular cast irons subjected to laser alloying with titanium (or titanium carbide) or overlay welds reinforces with ceramic particles [1, 10].

The effect of titanium alloying parameters on the morphology and the structure of a reinforced layer

The laser alloying of surfaces involving the direct injection of powder into the liquid metal pool enables the making of surface layers reinforced with titanium carbide particles and characterised by the relatively uniform distribution of the reinforcing phase in the matrix [8]. In the above-named method, the enrichment of the phase is usually performed in several runs, i.e. by making a few overlapping beads. The shape of the beads depends on process parameters [1, 8, 12].

The transport of the material in the liquid metal pool and the resultant distribution of alloying agent particles in the run depend on the intensity (rate) and the type of the liquid flow in the melted layer [1, 12]. An increase in laser power is accompanied by an increase in the liquid flow rate in the molten layer, leading to narrower and deeper fusion [1, 8]. The bead obtained in the laser alloying process is semi-circular in cross-section (in comparison with that obtained in the laser melting process). The foregoing results from adding (for instance) titanium powder to the liquid metal pool, leading to a decrease in convection intensity [1, 12]. In addition, the cross-sectional area of the beam obtained using the laser alloying method was smaller than that obtained using the laser melting technique [1]. Adding a larger amount of titanium powder during the laser alloying of surfaces increased the geometrical dimensions of bead [12].

The microstructure of the nodular cast iron surface layer alloyed with titanium contained TiC particles [1, 12], the morphology and fraction of which depend on the amount of laser power-affected titanium powder supplied to the liquid metal pool [1,8]. An increase in titanium concentration changed the morphology of TiC from cubic to dendritic, which means that it is possible to control the shape of titanium carbide particles by changing the content of Ti. The size of the particles changed from the synthesis boundary to the bead surface (triggered by changes of local solidification conditions) [1, 12]. An excessively high titanium powder feed rate in relation to given power density led to non-homogenous composition in resulted in the formation of micro-cracks and porosity. The micro-cracks resulted from the incomplete dissolution of graphite globules. The susceptibility of single beads to cracking decreased along with the increasing amount of titanium [1].

The microstructure of the nodular cast iron surface layer alloyed with titanium also contained austenite dendrites [12] (which partly transformed into martensite and cementite) as well as ledeburite near the fusion line [1]. In relation to a constant heat input and travel rate, the content of cementite in the layer decreased along with an increase in the titanium content (as a result of an increase in the TiC fraction). At the same time it was possible to observe an increase in the fraction of retained austenite. In turn, an increase in the travel rate combined with the constant power feed rate and a constant heat input were accompanied by a clearly noticeable increase in the amount of retained austenite. The above-named change could be attributed to a change in the content of carbon in the primary grains of austenite, triggered by the various degree of cooling. In addition, faster cooling, responsible for the increased content of carbon in austenite, inhibited the martensitic transformation. The foregoing implies that the application of lower travel rates could reduce the rate of cooling. Such a solution would favour the increased content of martensite in the surface layer structure, which, in turn, could provide better support of TiC reinforcing particles during tribological wear [1].

Objective and scope of tests

The tests aimed to identify the microstructure and the hardness of surface layers made of nodular cast iron GJS-350 using the laser alloying method.

The scope of the tests included the following activities:

- making a surface layer enriched with an alloying agent (titanium),
- macro and microscopic metallographic tests,
- hardness measurements (μHV 0.5) in the bead and deep inside the material.

Test materials

Base material

The test base material was nodular cast iron GJS-350-22. The properties and the chemical composition of the cast iron are presented in Table 1.

Table 1. Properties and chemical composition of nodular cast iron GJS-350-22

GJS-350-22					
Mechanical properties (at 22°C)					
Tensile strength Rm, MPa		Yield point Rp0.2; MPa		Elongation A, %	
350		220		22	
Chemical composition (% by weight)					
C	Si	Mn	P	Mg	S
3.5–3.8	2–3	0.4	0.1	0.06–0.12	0.01

Alloying material

The alloying agent used in the tests was titanium in the form of powder characterised by a purity of 99.8% (AMPERIT 154, H.C. Starck GmbH) and particle size restricted within the range of 45 μm to 75 μm.

Laboratory equipment used in the tests

Crystalline disc laser

The surface layer of the nodular cast iron was made using a TruDisk 3302 disc laser (Trumpf), the technical parameters of which are presented in Table 2.

Table 2. Technical parameters of the Trudisk 3302 disc laser (Trumpf)

Laser technical parameters	
Nominal output power (continuous radiation), W	3300
Output power adjustment, W	80 – 3300
BPP, mm/mrad	8
Nominal power stability	±1%
Radiation wavelength , nm	1030
Focal length, mm	200
Beam focus diameter, μm	200

Olympus SZX-9 microscope

The macrostructural tests were performed using an Olympus SZX-9 stereoscopic microscope (Fig. 3) enabling observation in the bright field.

Eclipse MA 100 inverted microscope

The macrostructural tests were performed using an Eclipse MA 100 microscope (Nikon), i.e. an inverted laboratory metallographic microscope designed for operation in reflected light and enabling observations in the white light in the bright field and in simple polarisation. The CFI 60 series objective lenses provide sharp high-resolution and high-contrast images (in comparison with traditional 45 mm optical systems). The microscope used in the tests was equipped with five revolving objective lenses.

Vickers 401 MVD microhardness tester

Hardness measurements were performed using a Vickers 401 MVD microhardness tester (Wolpert-Wilson). The technical specification of the microhardness tester is presented in Table 3. The device makes it possible to perform Vickers, Brinell and Knoop hardness tests.

Table 3 Technical parameters of the 401 MVD microhardness tester

Microhardness tester specification	
Force unit	gram-force, mN
Force control	automatic
Types of tests	HV/HB/HK
Scale	25 scales
Standards	ISO/ASTM
Motor power	3 W
Power supply	100V AC, 50/60 Hz

Tests

Laser alloying process

The titanium-enriched surface layer of the nodular cast iron was made using the multi-run method (30% overlap) and a constant laser beam power of 1500 W. The beam focus (80 μm) was located 35 mm above the specimen surface. The alloying rate amounted to 0.075 m/min. The powder was fed at a rate of 3 g/min. The powder was injected into the liquid metal pool using carrier gas (Ar). The flowrate of the carrier gas amounted to 2 l/min; the gas nozzle diameter amounted to 2 mm. The shielding gas used in the process was argon. The flowrate of the shielding gas amounted to 20 l/min; the nozzle diameter amounted to 20 mm.

Metallographic tests

At the first stage, the metallographic tests involved the sampling of specimens. Afterwards, the specimens were included and subjected to grinding and polishing (performed using felt grinding discs and diamond slurry having a granularity of 3 μm (Metkon DIAPAT-M 39-421-M) and 1μm (Mekton DIAPAT-M 39-411-M). The polishing of the specimens was performed using a Saphir 250M2 stationary grinder/polisher (ATM). To reveal their microstructure, the specimens were etched in Nital. The microstructure of the surface layer was observed at a magnification of 100x, 200x and 500x. The microstructural photographs, presented in Figures 2–6, show the structure of the newly formed layer and the microstructure of the HAZ. The photographs are discussed in detail in the remainder of the article.

The macrostructural tests were performed using the Olympus SZX-9 microscope. The photograph of the macrostructure of the alloyed layer (Fig. 7) was used to assess the geometry of the layer as well as to identify imperfections (if any). The photograph presents overlapping laser alloyed beads.

Microhardness measurements

The 10 second-long microhardness tests were performed under a load of 0.5 kg. The first bead was subjected to a series of 8 measurements

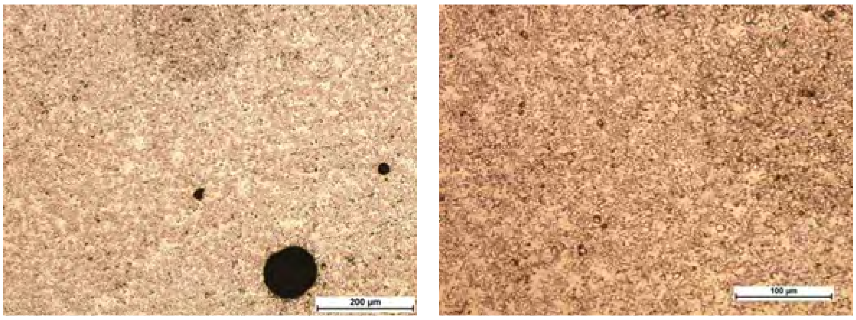

Fig. 2. Microstructure of the titanium carbide-reinforced composite layer; mag.

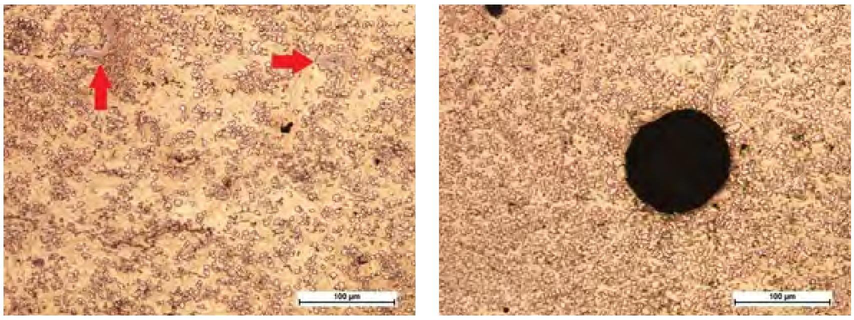

Fig. 3. Microstructure of the layer: a) lower number of inclusions and irregular carbide precipitates (indicated using the arrows) and b) visible void

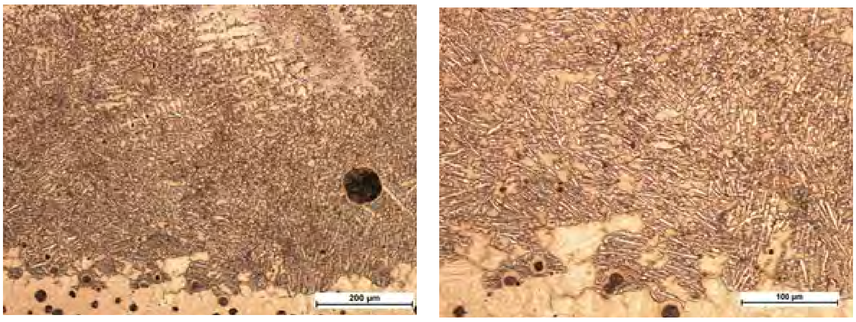

Fig. 4. Microstructure near the fusion line: a) mag. 100x and b) mag. 200x

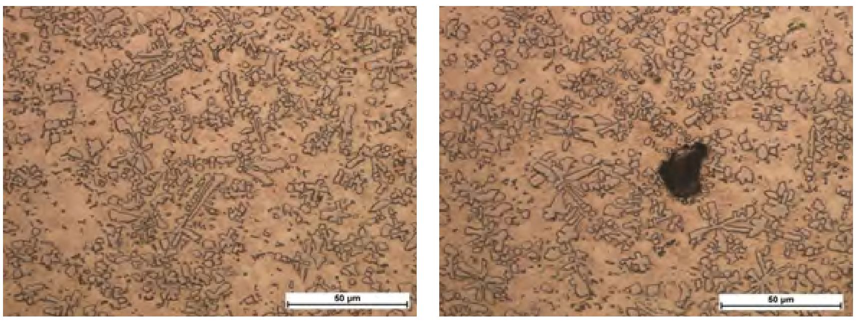

Fig. 5. Microstructure of the layer; mag. 500x

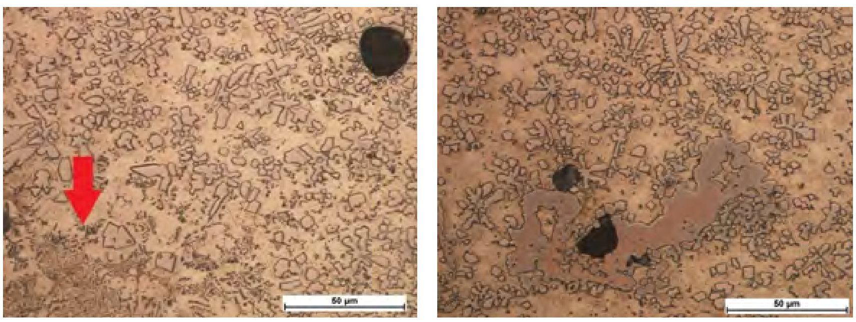

Fig. 6. Microstructure: a) visible eutectic carbides (indicated with the arrow); mag. 500x and b) irregular carbide precipitates; mag. 500x

Fig. 7. Macrostructure of the layer

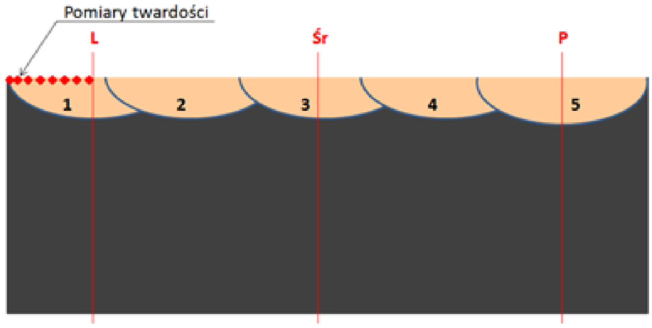

Fig. 8. Schematic diagram of microhardness measurements concerning the first bead (marked with red points) and 3 series (10 measurements deep inside the material: 1–5 – numbers of beads, R, L, M – cross-sections of measurements deep inside the material

(from the centre of the fusion zone) and a series of 3 measurements deep in the material as well as in 3 various cross-sections (extreme right bead ®, extreme left bead (L) as well as the middle bead (M)). The measurements aimed to identify the hardness of the heat affected zone (HAZ) and compare the hardness of the obtained layer with that of the base material. The schematic diagram of microhardness measurements is presented in Figure 8.

The microhardness measurement results are presented as line graphs in Figures 9 and 10. The first graph (Fig. 9) presents the distribution of hardness in the first bead, in relation to the distance from the fusion zone (FZ). In turn, Figure 10 presents the distribution of hardness deep inside the material.

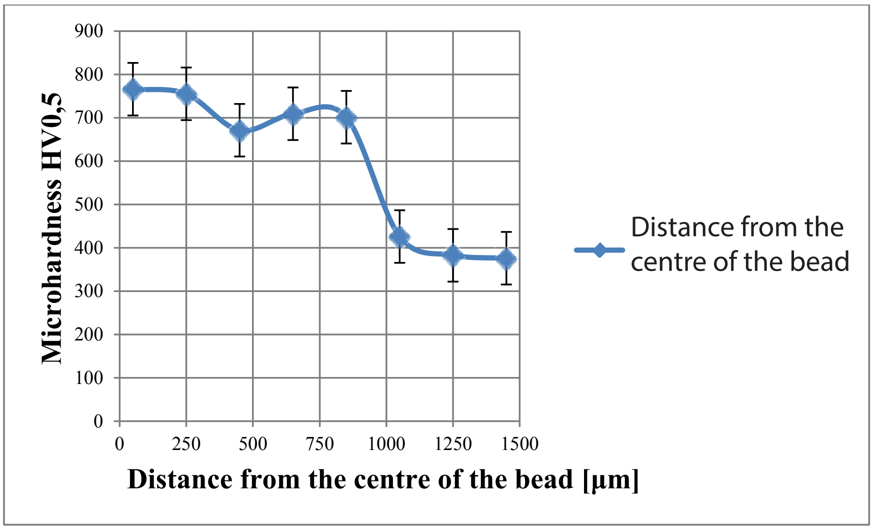

Fig. 9. Distribution of microhardness in the first bead – in relation to the distance from the centre of the fusion zone (FZ)

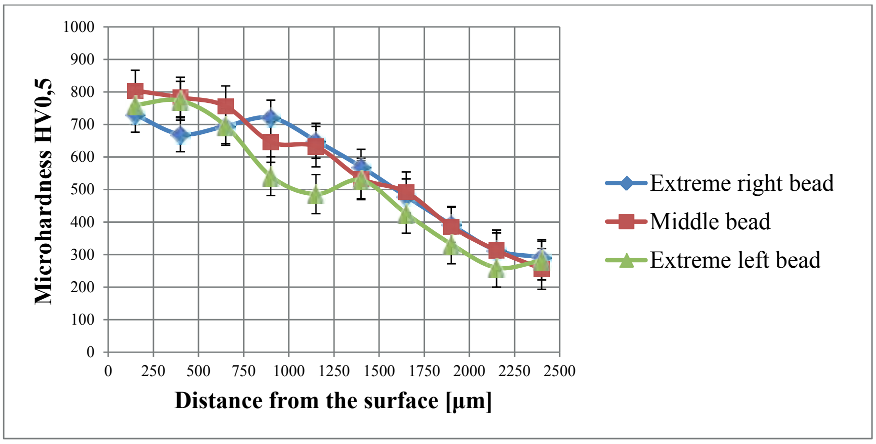

Fig. 10. Distribution of microhardness in the individual beads in relation to the distance from the surface

Analysis of results

The macrostructural photograph (Fig. 7) enabled the assessment of the geometry of the layer (made using the melt-in te4chnique). The cross-section revealed the semi-circular shape of the beads, resulting from the manner of heat discharge. The thickness of the layer amounted to approximately 1.65 mm. The above-named photograph presents the overlaps of individual beads. The analysis of Figure 7 also revealed the presence of a gas pore (marked with the arrow). No other imperfections (apart from the above-named pore) were observed.

The microstructural photographs revealed that the structure obtained through alloying was fine-crystalline and consisted of carbide precipitates (crystallising as first) in the matrix of austenite (see Figures 2, 3 and 5). The structure was characterised by high homogenisation resulting from the convective movements of the liquid metal in the pool (leading to the mixing of the alloying material in the fusion zone). The shapes and dimensions of titanium carbides varied. Their morphology resulted primarily from the content of titanium and local solidification conditions [1, 8]. Figures 2a and 3b reveal a large empty space having a diameter of approximately 100 μm, also visible in the photograph of the macrostructure (Fig. 7). The photographs also reveal the presence of pores (Figures 2a, 3, 5 and 6) (characterised by significantly smaller directions). The pores were present in the areas characterised by graphite presence before melting. Around the pores it was possible to notice fine TiC precipitates as well as irregular titanium carbide precipitates, visible at a magnification of 200x in Figure 3a (marked with arrows) and at a magnification of 500x in Figure 6b. The above-named irregular precipitates resulted from the heterogeneity of the chemical composition (high concentration of carbon and titanium). This was the intermediate phase resulting from the incomplete melting of graphite (discussed by Janicki [1]). The observation of the microstructure also revealed the presence of eutectic titanium carbides (Fig. 6a), formed uniformly with austenite at the very end of the recrystallisation process. No major imperfections (except for fine porosity and heterogeneity) were observed. The structure of the layer did not contain any microcracks. The high homogeneity of the structure and the lack of major imperfections demonstrated the proper adjustment of alloying parameters. The microstructural tests also involved the taking of a photograph near the fusion line (Fig. 4). The aforesaid photograph revealed the ledeburitic structure (clearly visible bright cementite flakes) and the base material structure composed of graphite globules in the ferritic matrix. The shape of the fusion line was irregular, resulting from the varied chemical composition (presence of graphite).

The microhardness measurement results in relation to the distance from the centre of the fusion zone (FZ) are presented in Figure 9. The fusion zone microhardness was characterised by varied results. The reason for the above-named observation was the fluctuation of the chemical composition, resulting from convective movements and the rapid crystallisation of the liquid in the FZ [6]. The measurements revealed that the areas of lower homogeneity were characterised by lower hardness than that of the areas rich in TiC. The different values of the microhardness measurement results were also observed in relation to the base material, characterised by lower hardness in the areas richer in graphite (measurement results were particularly low near the graphite globules). The diagrams presented in Figure 9 and in Figure 10 also revealed that the hardness in the FZ was significantly higher than that in the HAZ. The analysis of Figure 10 revealed that the addition of titanium increased the hardness of the surface layer by approximately 2.5 times in comparison with that of the base material.

Concluding remarks

The analysis of the test results concerning the laser alloying of the surface layer of nodular cast iron justified the formulation of the following conclusions:

1. The laser alloying process enables the obtainment of fine-grained microstructures.
2. The TiC-reinforced composite layer made using the laser alloying process was characterised by high homogeneity, yet also by slight imperfections (gas voids).
3. The microhardness of the surface was significantly higher (approximately 2.5 time) than that of the base material.
4. Laser alloying enables the obtainment of thin layers (approximately 1.65mm in the case discussed in the article) combined with a slight increase in the dimensions of the workpiece.

References

[1] Janicki D.: Microstructure and Sliding Wear Behaviour of In-Situ TiC-Reinforced Composite Surface Layers Fabricated on Ductile Cast Iron by Laser Alloying. MDPI Materials, January 2018.

[2] Kotarska A.: Laser surface alloying of ductile cast iron with Ti + 5% W mixture. Welding Technology Review, 2019.

[3] Paczkowska M., Kinal G.: Badania nad stopowaniem laserowym warstw wierzchnich elementów cylindrycznych z żeliwa sferoidalnego. Inżynieria Materiałowa, 2013, no. 1, pp. 38–42.

[4] Janicki D.: Fabrication of High Chromium White Iron Surface Layers on Ductile Cast Iron Substrate by Laser Surface Alloying.Strojniškivestnik–Journal of Mechanical Engineering, 2017, vol. 63, no. 12, pp. 705–714.

[5] Radziejewska J.: Laserowa modyfikacja właściwości warstwy wierzchniej wspomagana nagniataniem. IPPT PAN, Warszawa 2011.

[6] Kusiński J.: Lasery i ich zastosowanie w inżynierii materiałowej. Wydawnictwo Naukowe „ Akapit", Kraków 2000.

[7] Dobrzański L.A., Dobrzańska-Danikiewicz A.D.: Obróbka powierzchni materiałów inżynierskich. Open Access Library, 2011, vol. 5.

[8] Janicki D.: In situ synthesis of titanium carbide in an iron matrix during diode-laser surface alloying of ductile cast iron. Materials and technology, 2017, no. 51, pp. 317–321.

[9] Materiały dydaktyczne AGH: Materiały kompozytowe. Część 2 (link: http://home.agh.edu.pl/~jrichert/KOMPOZYT_II.htm).

[10] Dyjak S.: Spaleniowa synteza nanoproszku węglika tytanu. Biuletyn WAT, 2009, vol. LVIII.

[11] Saternus M., Fornalczyk A., Dankmeyer-Łączny J.: Chemia ogólna dla metalurgów. Wydawnictwo Politechniki Śląskiej, Gliwice 2013.

[12] Kotarska A., The Laser Alloying Process of Ductile Cast Iron Surface with Titanium, Metals 2021, 11, 282 (doi: https://doi.org/10.3390/met11020282).